Synthesis and Characterization of Ternary $Sn_xGe_{1-x}Se$ Nanocrystals

Jannise J. Buckley, Federico A. Rabuffetti, Hannah L. Hinton, and Richard L. Brutchey*

Department of Chemistry and the Center for Energy Nanoscience and Technology, University of Southern California, Los Angeles, California 90089-0744, United States

* E-mail: brutchey@usc.edu

Experimental Details

General considerations. Tin(IV) iodide (SnI_4, Alfa Aesar, 95%), germanium(IV) iodide (GeI_4, Strem, 99.999%) and hexamethyldisilazane (HMDS, Aldrich, ≥99.0%) were all purchased and used without further purification. Dodecylamine (Alfa Aesar, ≥98%) was distilled from CaO prior to use. Nanocrystal syntheses were performed under nitrogen, in the absence of water and oxygen, using standard Schlenk techniques.

Synthesis of di-*tert*-butyl diselenide ($^tBu_2Se_2$). Di-*tert*-butyl diselenide was synthesized according to an improved version of a previously published method (see Block, E.; Birringer, M.; Jiang, W.; Nakahodo, T.; Thompson, H.; Toscano, P. J.; Uzar, H.; Zhang, X.; Zhu, Z. *J. Agric. Food Chem.* **2001**, *49*, 458-470). Briefly, magnesium turnings (10.75 g, 0.44 mol) were allowed to stir in diethyl ether (200 mL) under nitrogen. *tert*-Butyl bromide (50 mL, 0.44 mol) was added slowly under nitrogen to the ether solution and allowed to stir for 30 min, producing a gray solution. Selenium (31.74 g, 0.40 mol) was subsequently added and allowed to stir for an additional 30 min. The solution was chilled in ice and an aqueous solution of ammonium chloride (17 g, 0.33 mol dissolved in 50 mL distilled water) was slowly added in air. After 10 min, the excess solid magnesium was filtered off and the organic solution was isolated from the aqueous layer in a separatory funnel by combining with hexanes (50 mL), washing four times with additional aqueous ammonium chloride, and drying over magnesium sulfate. The organic solvents were removed by evaporation under reduced pressure to produce a pungent yellow-orange liquid. After vacuum distillation at 40 °C (0.05 mmHg), the product was characterized by ^1H, ^{13}C, and ^{77}Se NMR in $CDCl_3$. ^1H: δ = 1.46 (s); $\{^1H\}^{13}C$: δ = 41.7 (s), 32.5 (s); $\{^1H\}^{77}Se$: δ = 488 (s) ppm.

$Sn_xGe_{1-x}Se$ nanocrystal synthesis. In a typical synthesis, SnI_4 (0.2*x* mmol), GeI_4 (0.2(1-*x*) mmol) and dodecylamine (3.0 mL, 13.0 mmol) were added to a two-neck round-bottom flask fitted with a reflux condenser, stir bar, and rubber septum. The reaction was then heated (2 °C min^{-1}) to 95 °C and degassed to eliminate adventitious water and dissolved oxygen by cycling between vacuum and nitrogen three times. $^tBu_2Se_2$ (20 µL, 0.10 mmol) and HMDS (2.1 mL, 10 mmol) were quickly injected to the reaction flask via syringe and the temperature was then increased (4 °C min^{-1}) to 225 °C and the reaction was allowed to react for 4.75 h with stirring. After being cooled to room temperature, the reaction mixture was dissolved in 3 mL of dichloromethane and precipitated with 3 mL of ethanol, sonicated, and centrifuged (6000 rpm for 1 min) to

yield a black solid. Dispersion/precipitation was repeated three times with toluene (2 mL) and ethanol (1 mL) to yield the as-prepared product.

GeSe nanocrystal synthesis. Germanium selenide was synthesized using the same procedure used above without the addition of HMDS. Additionally, the ^{t}Bu$_2$Se$_2$ injection temperature was increased to 180 °C, rather than at 95 °C for the reactions to form ternary alloys. All purification steps were kept the same.

**Nanocrystal Characterization**

Energy dispersive X-ray spectroscopy (EDX). EDX spectra was collected on a JEOL JSM-6610 scanning electron microscope operating at 20 kV and equipped with an EDAX Apollo silicon drift detector (SDD). Multiple regions of a sample deposited on an aluminum stub were analyzed and averaged.

Powder X-ray diffraction (XRD). Conventional powder XRD patterns were collected in the 10–80° 2θ range using a Rigaku Ultima IV diffractometer operating at 44 mA and 40 kV. Cu Kα radiation (λ = 1.5406 Å) was employed. Diffraction patterns were recorded at 25 °C. Rietveld structural refinements were carried out using the General Structure Analysis System (GSAS) software.[1] Experimental data and atomic X-ray scattering factors were corrected for sample absorption and anomalous scattering, respectively. The Sn:Ge molar ratio was fixed as determined by energy dispersive X-ray analysis. The following parameters were refined: (1) scale factor, (2) background, which was modeled using a shifted Chebyschev polynomial function, (3) peak shape, which was modeled using a modified Thomson–Cox–Hasting pseudovoight function including an asymmetry parameter, (4) lattice constants, (5) fractional atomic coordinates, (6) an isotropic thermal parameter for each chemical species (*i.e.*, $U_{Sn,Ge}$, and U_{Se}), and (7) preferred orientation, which was modeled using the March-Dollase approach. The usual R_{wp} indicator was employed to assess the quality of the refined structural models.

Transmission electron microscopy (TEM). TEM was performed on a JEOL JEM-2100 microscope at an operating voltage of 200 kV, equipped with a Gatan Orius CCD camera. Samples were prepared from dilute purified dispersions in toluene and deposited onto 300 mesh Formvar-coated copper grids (Ted Pella, Inc.).

Diffuse Reflectance Spectroscopy. Diffuse reflectance measurements were collected on a Perkin-Elmer Lambda 950 equipped with a 150 mm integrating sphere. Samples were prepared by drop casting a solution of the nanocrystals in toluene on a glass substrate to form a thick film. The sample was then covered by a quartz window and the spectra were measured in reflectivity mode.
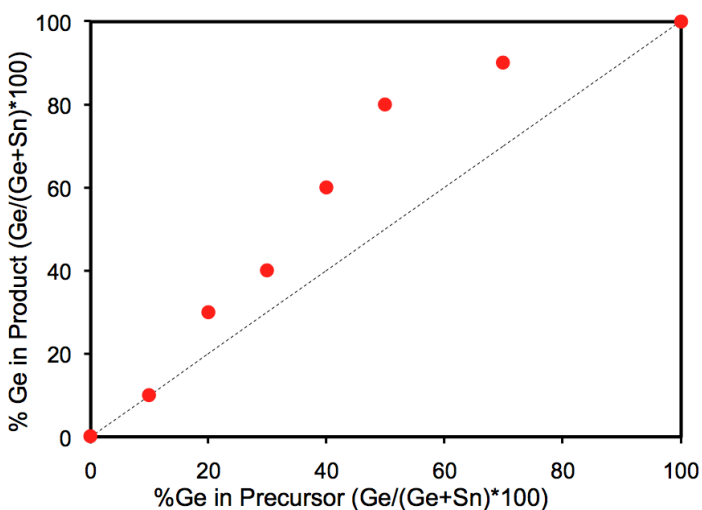
Additional Figures
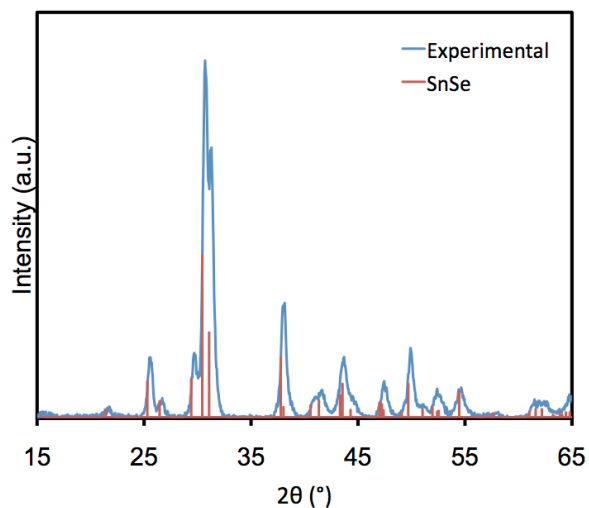
Figure S1. XRD pattern of nanocrystal product from a reaction containing a precursor Sn/Ge ratio of 3:2, performed without the addition of HMDS. The pattern is equivalent to that obtained when synthesizing SnSe using the current procedure and can be indexed to SnSe in the *Pnma* space group.
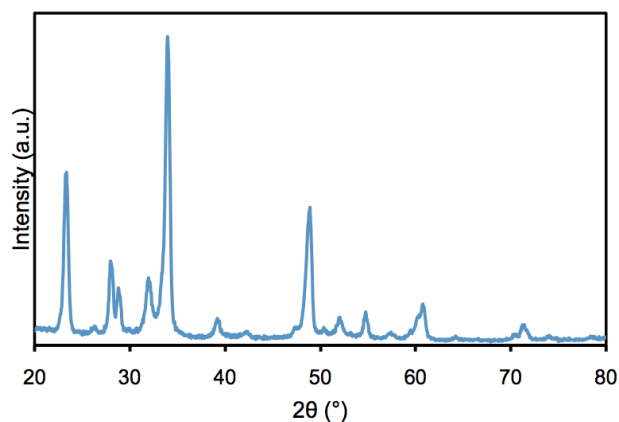

Figure S2. XRD pattern of the unknown GeSe product synthesized with HMDS. EDS confirmed a 1:1 Ge:Se stoichiometry.

**Table S1.** Estimated compositions determined using EDS.

Sample Denotation	Experimentally Determined Sn:Ge:Se ratio
SnSe	55:0:45
$Sn_{0.9}Ge_{0.1}Se$	47:5:48
$Sn_{0.7}Ge_{0.3}Se$	37:14:49
$Sn_{0.6}Ge_{0.4}Se$	30:22:48
$Sn_{0.4}Ge_{0.6}Se$	22:33:45
$Sn_{0.2}Ge_{0.8}Se$	11:44:45
$Sn_{0.1}Ge_{0.9}Se$	7:48:45

Figure S3. Elemental composition comparing the actual germanium incorporation in the isolated nanocrystals (measured by EDS) versus expected from precursor addition.
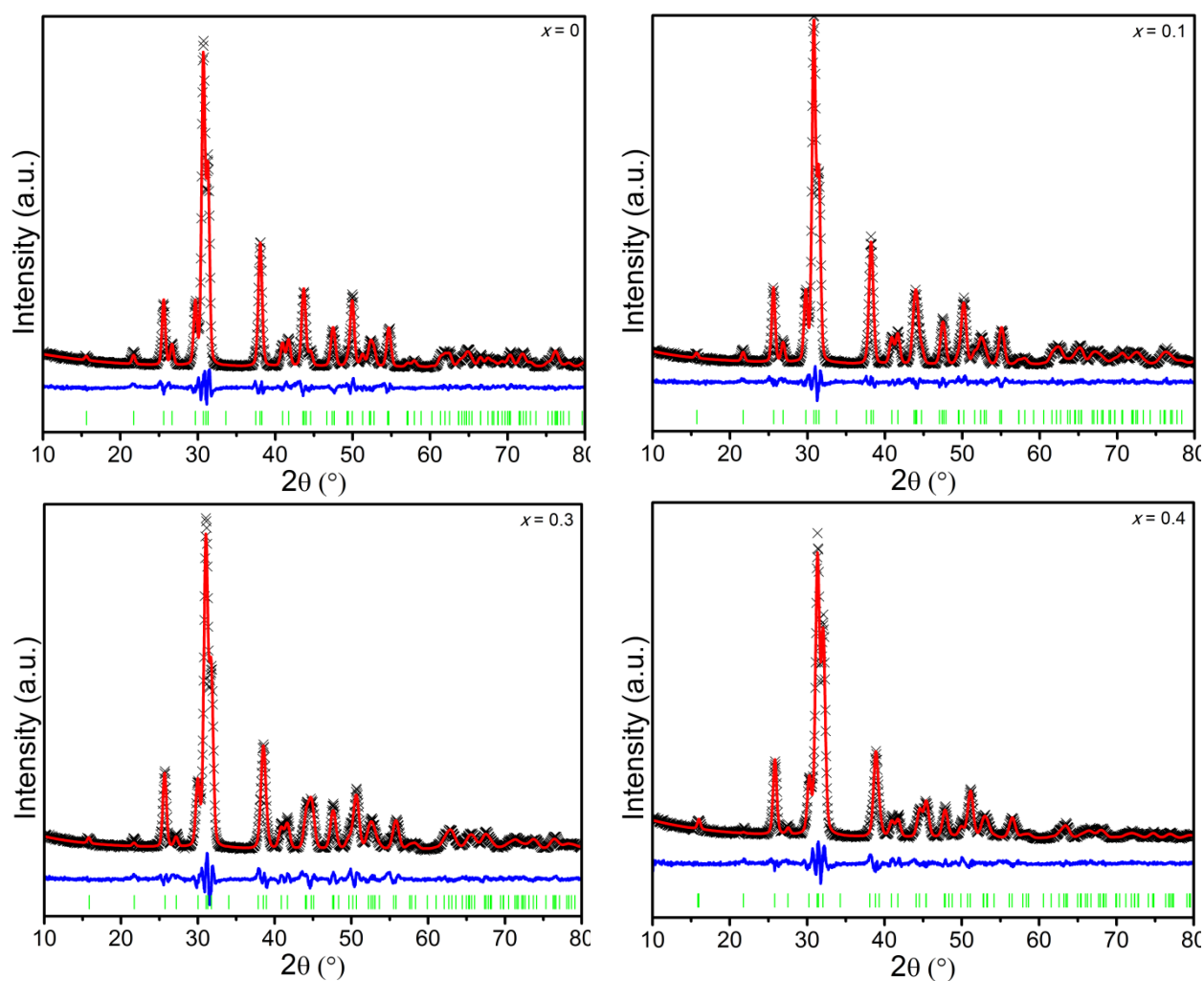
Figure S4. Rietveld analysis of XRD patterns of Ge$_x$Sn$_{1-x}$Se samples. Experimental (×) and calculated (—) patterns are shown for each sample along with the difference curve (—) and tickmarks (|) corresponding to the phase refined.
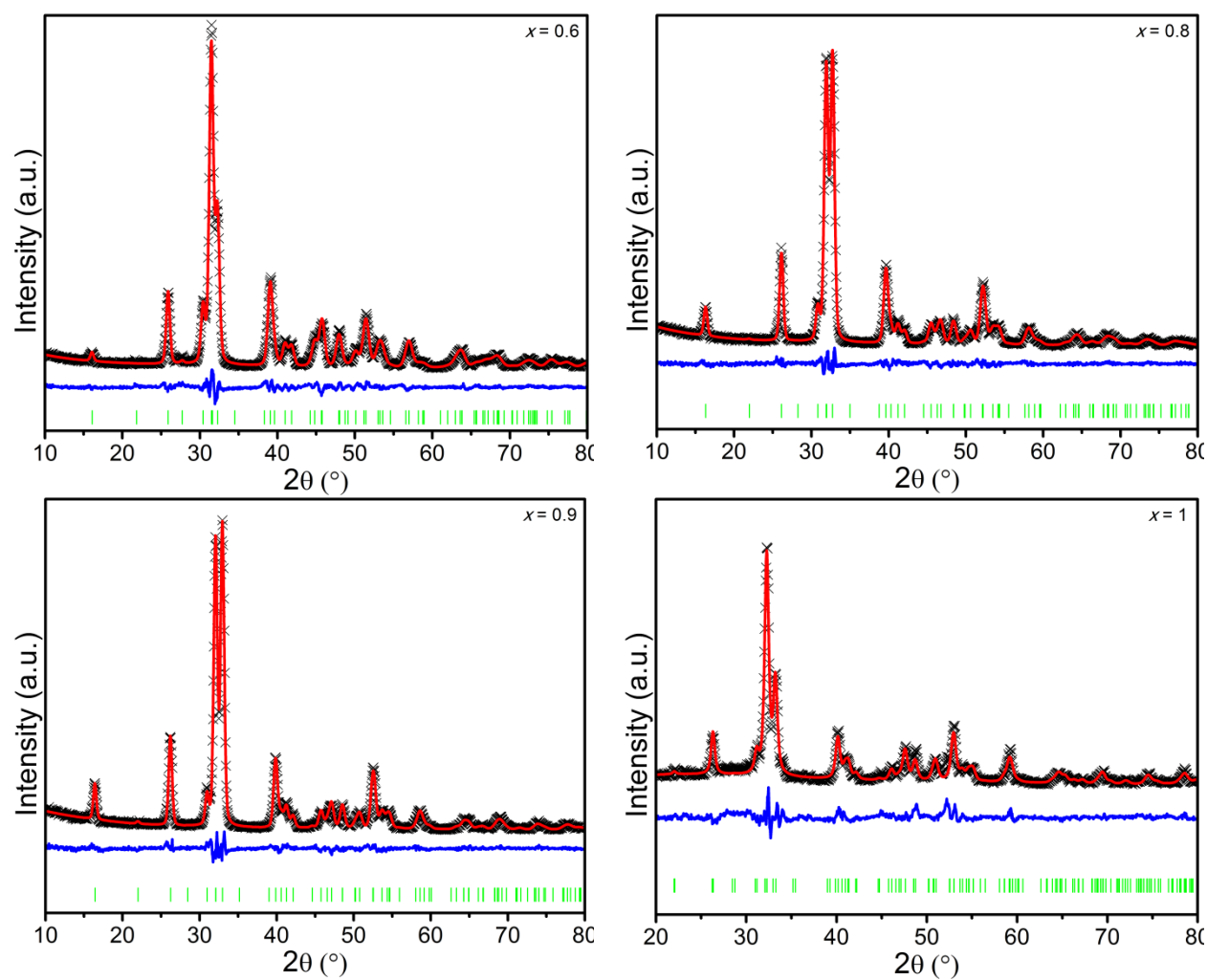
Figure S5. Rietveld analysis of XRD patterns of $Ge_xSn_{1-x}Se$ samples. Experimental (×) and calculated (—) patterns are shown for each sample along with the difference curve (—) and tickmarks (|) corresponding to the phase refined.

Table S2. Rietveld Analysis of X-ray Diffraction Data of $Ge_xSn_{1-x}Se$

x (mol. %)[a]	0	10	30	40	60	80	90	100
a (Å)	11.5040(9)	11.4470(9)	11.3441(14)	11.2474(13)	11.1705(13)	11.0101(9)	10.9371(8)	10.841(2)
b (Å)	4.1563(4)	4.1244(4)	4.0667(6)	4.0158(6)	3.9813(5)	3.9001(5)	3.8727(4)	3.8335(8)
c (Å)	4.4301(5)	4.4365(4)	4.4374(7)	4.4348(8)	4.4251(6)	4.4023(6)	4.3967(6)	4.3877(12)
V (Å^3)	211.82(4)	209.46(4)	204.73(6)	200.31(6)	196.80(5)	189.08(4)	186.23(4)	182.35(8)
$X_{Sn,Ge}$	0.1190(2)	0.1185(2)	0.1180(2)	0.1190(3)	0.1195(3)	0.1209(2)	0.1215(2)	0.1224(7)
$Z_{Sn,Ge}$	0.8994(5)	0.8979(4)	0.8927(6)	0.8894(6)	0.8882(5)	0.8914(5)	0.8917(5)	0.8847(13)
X_{Se}	0.8557(3)	0.8543(3)	0.8549(4)	0.8550(4)	0.8543(3)	0.8540(2)	0.8540(2)	0.8514(6)
Z_{Se}	0.5149(7)	0.5152(5)	0.5145(7)	0.5103(7)	0.5064(5)	0.5031(6)	0.5000(6)	0.4908(12)
$U_{Sn,Ge}$ (Å^2)[b]	2.37(12)	2.15(10)	2.12(15)	5.60(16)	3.27(13)	6.13(14)	6.20(14)	2.3(3)
U_{Se} (Å^2)[b]	2.52(17)	2.38(14)	2.44(19)	5.34(19)	3.17(15)	4.98(14)	5.19(15)	0.4(3)
R_{wp}	8.7	6.2	9.2	8.0	6.8	4.9	6.5	13.0

[a] Ge fraction extracted from energy dispersive X-ray analysis.
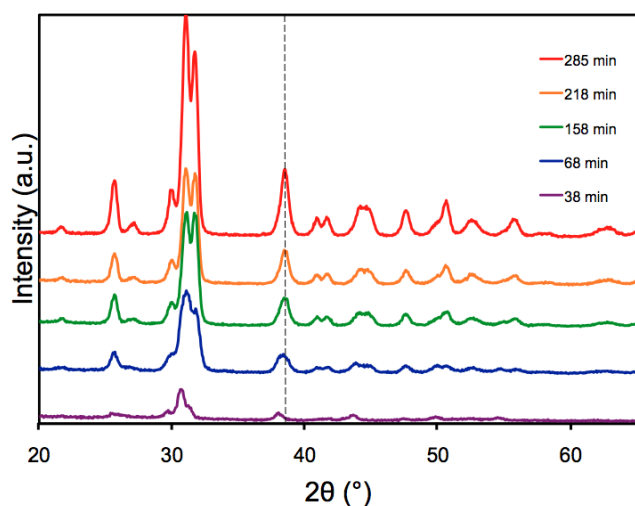[b] Given as $100 \times U$.
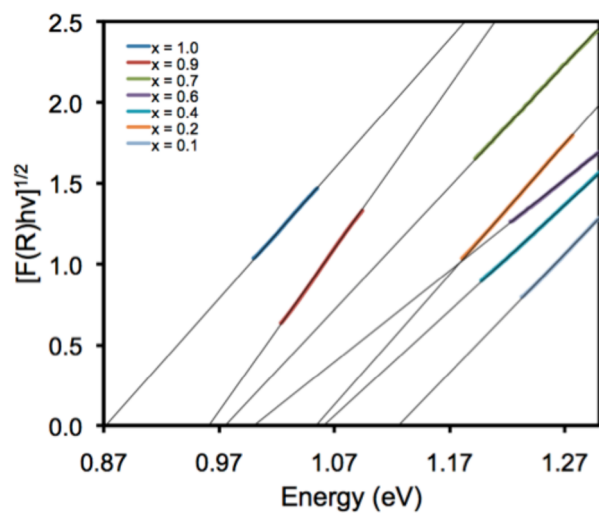
Figure S6. Tauc plot of the linear regions from $[F(R)h\nu]^{1/2}$ as a function of energy for the $Sn_xGe_{1-x}Se$ alloys showing the fits used to obtain the indirect band gap energies.
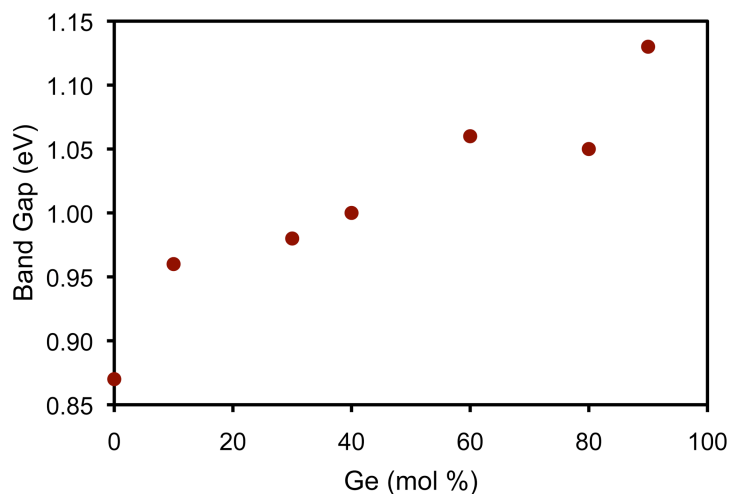


**Figure S7.** Calculated indirect band gaps ($[F(R)h\nu]^{0.5}$) as a function of alloy composition.

Figure S8. Timed aliquot XRD patterns taken when using a SnI_4/GeI_4 ratio of 4:1. A gradual shift to higher 2θ values is observed as the reaction proceeds to completion (*ca.* 150 min). After 4.75 h, the XRD pattern matches that expected from nanocrystals with an approximate $Sn_{0.6}Ge_{0.4}Se$ composition.
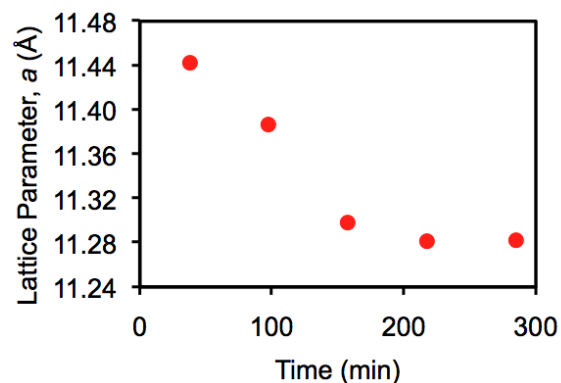
Figure S9. Lattice parameter *a* as a function of time taken from timed aliquot XRD patterns when using a SnI_4/GeI_4 ratio of 4:1.
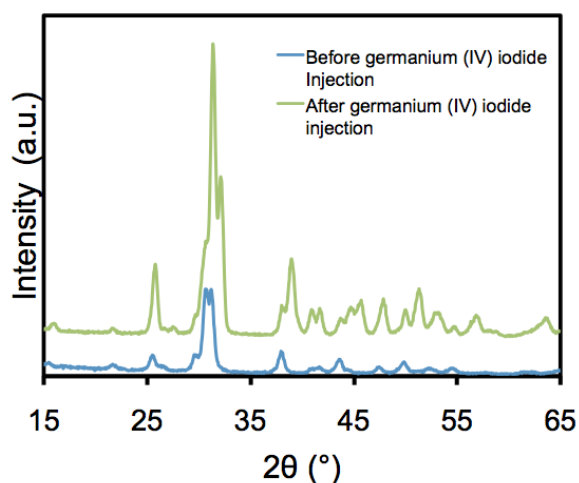
Figure S10. XRD patterns of the nanocrystal products taken when first synthesizing SnSe (blue pattern) and after injection of GeI_4 to the SnSe nanocrystal product (total Sn/Ge ratio of 3:2, green pattern). The XRD pattern of the resulting nanocrystals matches closely to that obtained in the typical alloy synthesis when using a SnI_4/GeI_4 ratio of 3:2, with a small fraction of unconverted SnSe.
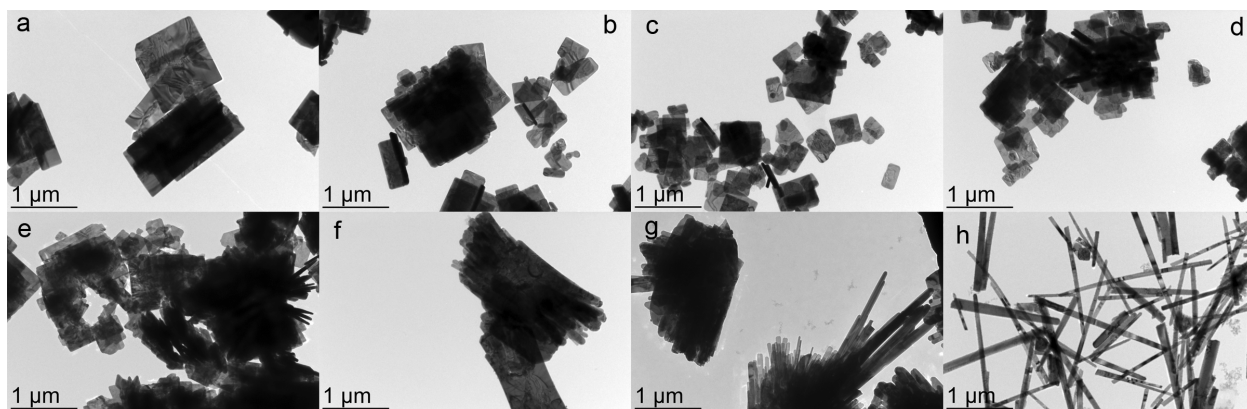
Figure S11. TEM images of $Sn_xGe_{1-x}Se$ nanocrystals showing the compositionally dependent morphology change for: (a) SnSe, (b) $Sn_{0.9}Ge_{0.1}Se$, (c,d) $Sn_{0.7}Ge_{0.3}Se$, (e) $Sn_{0.6}Ge_{0.4}Se$, (f) $Sn_{0.4}Ge_{0.6}Se$, (g) $Sn_{0.2}Ge_{0.8}Se$, and (h) $Sn_{0.1}Ge_{0.9}Se$.

References

1. Larson, A. C.; Von Dreele, R. B. *General Structure Analysis System (GSAS)*, Los Alamos National Laboratory, 2000.